Journal of Radiation Research, Vol. 58, No. 6, 2017, pp. 854–861
doi: 10.1093/jrr/rrx040
Advance Access Publication: 15 July 2017

Preliminary comparison of the registration effect of 4D-CBCT and 3D-CBCT in image-guided radiotherapy of Stage IA non–small-cell lung cancer

Zhibo Tan[1,2], Chuanyao Liu[3], Ying Zhou[4] and Weixi Shen[1,*]

[1]Department of Oncology, Shenzhen Hospital of Southern Medical University, #1333 Xinhu Road, Bao'an District, Shenzhen 518110, Guangdong Province, PR China
[2]Department of Radiation Oncology, Sichuan Cancer Hospital, #55 Renmin Road South, Wuhou District, Chengdu 610041, Sichuan Province, PR China
[3]Department of Rehabilitation, Shenzhen Hospital of Southern Medical University, #1333 Xinhu Road, Bao'an District, Shenzhen 518110, Guangdong Province, PR China
[4]Department of Oncology and Hematology, Shenzhen Hospital of Southern Medical University, #1333 Xinhu Road, Bao'an District, Shenzhen 518110, Guangdong Province, PR China
*Corresponding author. Department of Oncology, Shenzhen Hospital of Southern Medical University, #1333 Xinhu Road, Bao'an District, Shenzhen 518110, Guangdong Province, PR China. Email: kenbaines@163.com
Received December 28, 2016; Revised April 4, 2017; Editorial Decision June 25, 2017

ABSTRACT

In this study, we compared the registration effectiveness of 4D cone-beam computed tomography (CBCT) and 3D-CBCT for image-guided radiotherapy in 20 Stage IA non–small-cell lung cancer (NSCLC) patients. Patients underwent 4D-CBCT and 3D-CBCT immediately before radiotherapy, and the X-ray Volume Imaging software system was used for image registration. We performed automatic bone registration and soft tissue registration between 4D-CBCT or 3D-CBCT and 4D-CT images; the regions of interest (ROIs) were the vertebral body on the layer corresponding to the tumor and the internal target volume region. The relative displacement of the gross tumor volume between the 4D-CBCT end-expiratory phase sequence and 4D-CT was used to evaluate the registration error. Among the 20 patients (12 males, 8 females; 35–67 years old; median age, 52 years), 3 had central NSCLC and 17 had peripheral NSCLC, 8 in the upper or middle lobe and 12 in the lower lobe (maximum tumor diameter range, 18–27 mm). The internal motion range in three-dimensional space was 12.52 ± 2.65 mm, accounting for $47.8 \pm 15.3\%$ of the maximum diameter of each tumor. The errors of image-guided registration using 4D-CBCT and 3D-CBCT on the x (left–right), y (superior–inferior), z (anterior–posterior) axes, and 3D space were 0.80 ± 0.21 mm and 1.08 ± 0.25 mm, 2.02 ± 0.46 mm and 3.30 ± 0.53 mm, 0.52 ± 0.16 mm and 0.85 ± 0.24 mm, and 2.25 ± 0.44 mm and 3.59 ± 0.48 mm (all $P < 0.001$), respectively. Thus, 4D-CBCT is preferable to 3D-CBCT for image guidance in small pulmonary tumors because 4D-CBCT can reduce the uncertainty in the tumor location resulting from internal motion caused by respiratory movements, thereby increasing the image-guidance accuracy.

KEYWORDS: 4D-CBCT, Stage IA non–small-cell lung cancer, image-guided radiotherapy, 3D-CBCT, registration

INTRODUCTION

Radiotherapy is an important treatment modality for lung cancer. Among the new cases of lung cancer discovered using low-dose spiral computed tomography (CT) screening, more than 80% of cases are Stage I lung cancer [1–3], and the local control rate in early-stage lung cancer is up to 90% [4]. Delivery accuracy is a crucial issue to consider when performing radiotherapy on small pulmonary lesions. As image guidance is a key technique in radiotherapy, it has been regarded as the most important factor determining the delivery accuracy of pulmonary radiotherapy in lung cancer [5].

Among the different modalities available, 3D-CBCT is the conventional method used in image guidance. However, the internal motions of the tumor and the normal organs caused by respiratory movements could have a significant impact on the delivery accuracy of radiotherapy [6]. Furthermore, the acquisition time of 3D-CBCT is longer than one breath cycle, which adversely affects the clarity of the acquired images. This is particularly true for small-sized tumors and tumors adjacent to the diaphragm, which have large ranges of internal motion, resulting in blurring of the image boundaries [7] and reduced accuracy of image guidance.

To address these problems, 4D-CBCT based on respiratory movements has recently been applied clinically [8]. Although 4D-CBCT can provide additional data related to respiration, it remains unclear whether these data can be translated into enhanced radiotherapy accuracy. The few model simulation studies and clinical trials [7, 9–11] that have investigated this issue have arrived at different conclusions. Moreover, 4D-CBCT still has the following drawbacks: (i) The duration of 4D-CBCT is longer than that of 3D-CBCT, which increases the inconsistency between image guidance and radiotherapy implementation; (ii) significantly more data are acquired by 4D-CBCT than by 3D-CBCT, which increases the complexity of data processing; (iii) when performing 4D-CBCT image registration, the image sequences, target ROI, and registration methods (automatic or manual registration, clip box or mask) vary between different research institutes [7, 10, 12, 13], and a standardized procedure is still lacking; and (iv) 4D-CBCT might increase the radiation exposure of the patient [14].

Current studies on 4D-CBCT are rare and their results are inconsistent. For example, in a simulated model and in eight patients, Hugo *et al.* observed that 4D-CBCT and 3D-CBCT were equally effective at increasing the accuracy of radiotherapy [9]. In contrast, Sweeney *et al.* performed a retrospective analysis of 21 lung cancer patients and found that 4D-CBCT increased the accuracy of image guidance more than 3D-CBCT did [7].

In view of these inconsistencies in the present body of knowledge, this study was designed to compare the effectiveness of image registration in 4D-CBCT with that in 3D-CBCT, when they were used for online image guidance during radiotherapy in patients with small pulmonary tumors. Our aim was to provide additional evidence for the clinical applications and value of 4D-CBCT.

MATERIALS AND METHODS

Ethical considerations

This study was approved by the Ethical Review Committee of the Shenzhen Hospital of Southern Medical University (Approval No. ERC-SZH-20162), and written informed consent was obtained from all patients before they were enrolled. Good clinical practice guidelines, the Declaration of Helsinki, and local laws were complied with throughout the study.

Patient characteristics

This study included 20 consecutive patients, from March 2014 to June 2016, with Stage IA non–small-cell lung cancer (NSCLC) who were medically inoperable or unwilling to undergo surgery and hence received stereotactic ablative radiotherapy (SABR). Of these 20 patients, 12 were males and 8 were females; they were aged between 35 and 67 years, with a median age of 52 years; 8 cases presented with tumors in the upper or middle lobe and 12 in the lower lobe; 3 cases presented with central NSCLC and 17 with peripheral NSCLC. Of these 17 peripheral NSCLC patients, 9 had tumors located >1 cm from the chest wall, and 8 of the 17 had tumors located ≤1 cm from the chest wall. The maximum tumor diameter was between 18 and 27 mm among 20 patients. Of the 20 patients, 13 had normal pulmonary function, 5 had mild impairments, 1 had moderate impairments, and 1 had severe impairments (see Table 1.) Patients with peripheral lesions that were located >1 cm from the chest wall ($n = 9$) received 54 Gy in 3 fractions, and patients with peripherally located lesions ≤1 cm from the chest wall ($n = 8$) or central lesions ($n = 3$) received 50 Gy in 4 fractions.

Image acquisition and tumor motion analysis

The patients lay down in a supine position, with hands raised and crossed above the head, after which their positions were fixed by low-temperature thermoplastic membrane fixation (Klarity Medical Products, Ohio, US) and a MultiFix™ Baseplate (Klarity Medical Products, Ohio, US). Then a Philips Big Bore 16 spiral CT scanner (Philips, UK) was used to acquire 10 image sequences at different respiratory phases during abdominal breathing (scanning conditions: 120 kV, 200 mA and slice thickness of 3 mm). The amplitude

Table 1. Characteristics of 20 Stage IA NSCLC patients in this study

Characteristics	
Gender (n)	
Male	12
Female	8
Age (years)	35–67 (median: 52)
Location[a] (n)	
Central	3
Peripheral (>1 cm from chest wall)	9
Peripheral (≤1 cm from chest wall)	8
Location (n)	
Upper/Middle lobe	8
Lower lobe	12
Pulmonary function (n)	
Normal	13
Mild impairments	5
Moderate impairments	1
Severe impairments	1

[a]Central or peripheral location is based on the RTOG definition.

of the tumor motion was determined by measuring the tumor movement in the 10-phase 4D-CT sequences using the Pulmonary Toolkit for Oncology Software (Philips, UK). The motion ranges of the tumor centroid in the left–right, superior–inferior and anterior–posterior directions were measured on the frontal, vertical and sagittal axis for all 10 phase sequences registered by this software.

Treatment planning design

The 10 image sequences were transferred to the Monaco planning system (Elekta, Stockholm, Sweden), and the gross tumor volume (GTV) was outlined in the sequence image at the end-expiratory phase, where breathing motion and motion artefacts are expected to be smallest [6]. The GTVs outlined in the 10 sequence images were projected onto the end-expiratory phase and combined to form the internal target volume (ITV). The ITV was expanded outward by 5 mm to form the planning target volume (PTV). Monte Carlo dose calculation was performed on the sequence images at the end-expiratory phase to obtain the required dose. The images, which included end-expiratory phase sequences containing the GTV, ITV and PTV outlines, were transferred to the X-ray Volume Imaging system (XVI, version 4.5). The patients then received image-guided radiotherapy using an Elekta Axesse linear accelerator equipped with kilovolt CBCT (Elekta, Sweden).

Implementation of image guidance

For each patient, 4D-CBCT and 3D-CBCT were performed immediately before radiotherapy treatment (scanning conditions: rotation angle was 200°; tube voltage was 120 kV; tube current was 20 mA; filter type was S20; slice thickness was 3 mm; 1320 frames were acquired within 4 min at the rate of 16 ms per frame). The images acquired using 4D-CBCT were divided into 10 sequences on the basis of the different respiratory phases, and XVI was used to superimpose the 10 image sequences to form a composite image sequence. As the acquisition time of CBCT is relatively long, the images acquired using 3D-CBCT can be regarded as imaging of the motion trajectory for the tumor and normal organs during the respiratory cycle. The image quality of the CBCT was evaluated by one radiation oncologist and one radiotherapy technician with more than 2 years' experience in IGRT for lung cancers, both of whom have good command of the XVI system. After the image quality of the CBCT was considered to be clear, without difficulties in registration, two methods of image registration were performed as described below.

Registration based on 4D-CBCT

A clip box was used to select the vertebral body on the layer corresponding to the tumor as the ROI. Next, automatic bone registration was performed for the 4D-CBCT and 4D-CT end-expiratory phase sequences. Then, the mask function was used to select images within the ITV region as the ROI, and automatic soft-tissue registration was performed on the 4D-CBCT composite image sequence and ITV. After registration, the relative displacement of the GTV between the 4D-CBCT end-expiratory phase sequence and the 4D-CT end-expiratory phase sequence was used to evaluate the accuracy of 4D-CBCT registration.

Registration based on 3D-CBCT

The same method was used to perform automatic bone registration of the 3D-CBCT and 4D-CT end-expiratory phase sequence images. The mask function was also used for automatic soft-tissue registration on the 3D-CBCT images and ITV. Then, the images of the 4D-CBCT end-expiratory phase sequence were displaced based on the 3D displacement data obtained from the automatic soft-tissue registration. The relative displacement of the GTV between the displaced 4D-CBCT end-expiratory phase sequence and 4D-CT was used to evaluate the accuracy of 3D-CBCT registration.

Figure 1 is a workflow showing the process of registration based on 4D-CBCT and 3D-CBCT briefly. The procedures were followed for the two representative cases described in Fig. 2.

Statistical methods

SPSS 22.0 statistical software was used to perform statistical analysis. Data were compared between the two groups by using paired-sample *t*-tests. $P < 0.05$ indicated statistical significance.

RESULTS

Range of internal motion of tumors

For each patient, 10 time-phase images were recorded using 4D-CT, which revealed the range of internal motions of the tumor for each 3D direction. The range of internal motions on the x (left–right), y (superior–inferior) and z (anterior–posterior) axes were 3.50 ± 0.54 mm, 10.67 ± 2.61 mm and 5.25 ± 1.75 mm, respectively. The 3D motion range was calculated as 12.52 ± 2.65 mm by using the equation $\sigma = \sqrt{x^2 + y^2 + z^2}$. The 3D motion range σ was expressed as a percentage of the maximum tumor diameter for each patient, and the average value was 47.8 ± 15.3% (see Table 2).

Relative displacement in 4D-CBCT and 3D-CBCT registration

The errors of image-guided registration on the x (left–right), y (superior–inferior) and z (anterior–posterior) axes for 4D-CBCT and 3D-CBCT were 0.80 ± 0.21 mm and 1.08 ± 0.25 mm ($P <$ 0.001), 2.02 ± 0.46 mm and 3.30 ± 0.53 mm ($P < 0.001$) and 0.52 ± 0.16 mm and 0.85 ± 0.24 mm ($P < 0.001$), respectively. The errors on three-dimensional space for 4D-CBCT and 3D-CBCT were calculated to be 2.25 ± 0.44 mm and 3.59 ± 0.48 mm ($P < 0.001$), respectively. The differences between all 4D-CBCT and 3D-CBCT values were statistically significant (see Table 3).

DISCUSSION

Improvement in the accuracy and reliability of dose delivery during radiotherapy is currently the predominant concern of clinicians. The internal motions of the tumor and normal organs caused by respiration significantly decrease the accuracy of thoracic and abdominal radiotherapy by increasing the uncertainty of the exact tumor

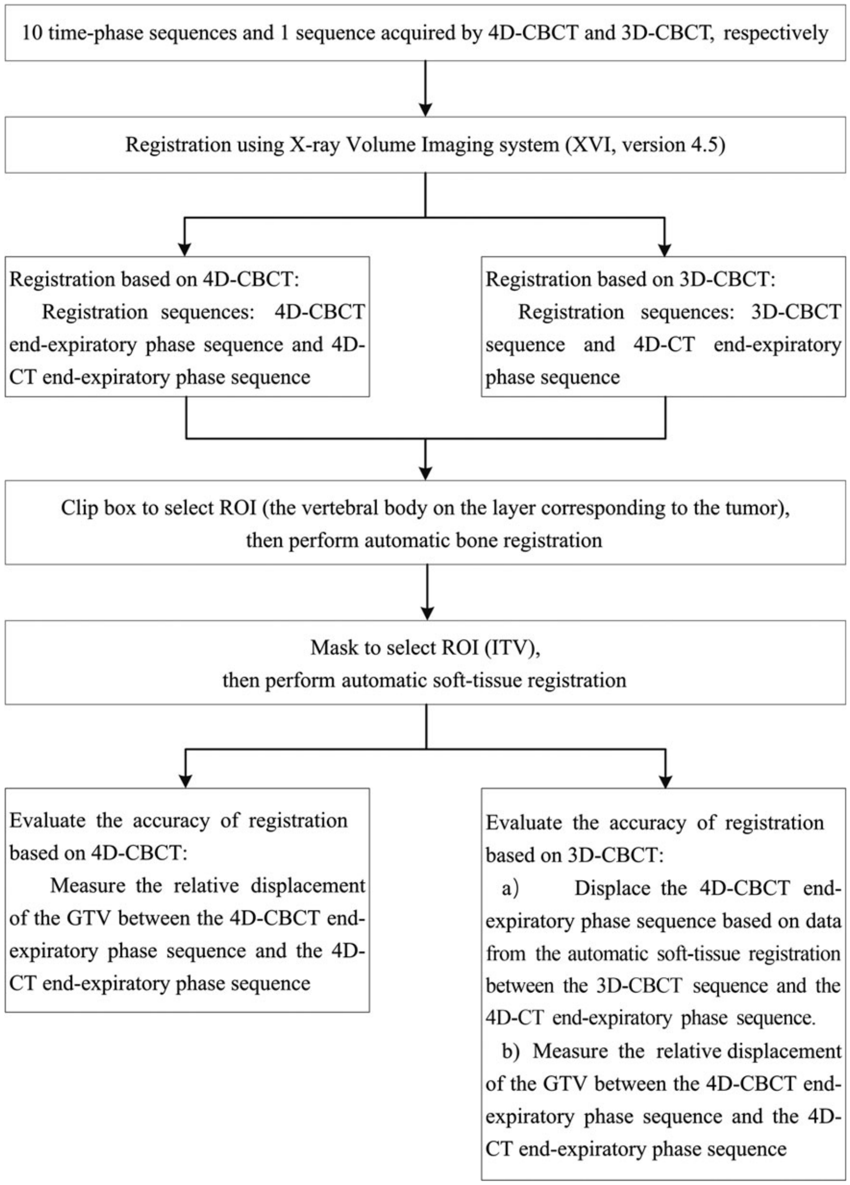

Fig. 1. Flow chart for registration based on 4D-CBCT and 3D-CBCT.

location [6]. To address this problem, several methods have been proposed, including active breathing control [15], gated radiotherapy [16], and dynamic tumor tracking. Among them, 4D-CT based on respiratory phases is the most commonly used method. It records the internal motions of the tumor and normal organs caused by respiratory movements in order to provide more data for outlining the ROI and performing dose calculations [17, 18]. Image guidance is a key technique that is widely used during the administration of radiotherapy. Combining 4D-CT with daily image guidance can shrink the PTV by 37–47%. Hence, it is regarded as the most effective management strategy for improving the reliability of dose delivery in the majority of lung cancer patients undergoing radiotherapy, by decreasing the uncertainty of the exact tumor location [19].

The present study was conducted in patients with Stage IA NSCLC who were medically inoperable or unwilling to undergo surgery. Prospective clinical trials have shown that in patients with medically inoperable Stage I NSCLC, the 3-year local control rate of SABR is >85% and the 3-year overall survival rate is 60% [4, 20–29]. This indicates that SABR is effective [24, 30–33]; therefore, it is the preferred treatment method in early stage NSCLC [4, 30, 34, 35]. Furthermore, because SABR uses short courses of very conformal and dose-intensive radiotherapy, radiation delivery needs to be precise [36–38]. Because of the small tumor size and relatively broad range of tumor motion in early-stage lung cancer, image guidance techniques that can improve treatment accuracy are urgently needed for optimal treatment of these patients.

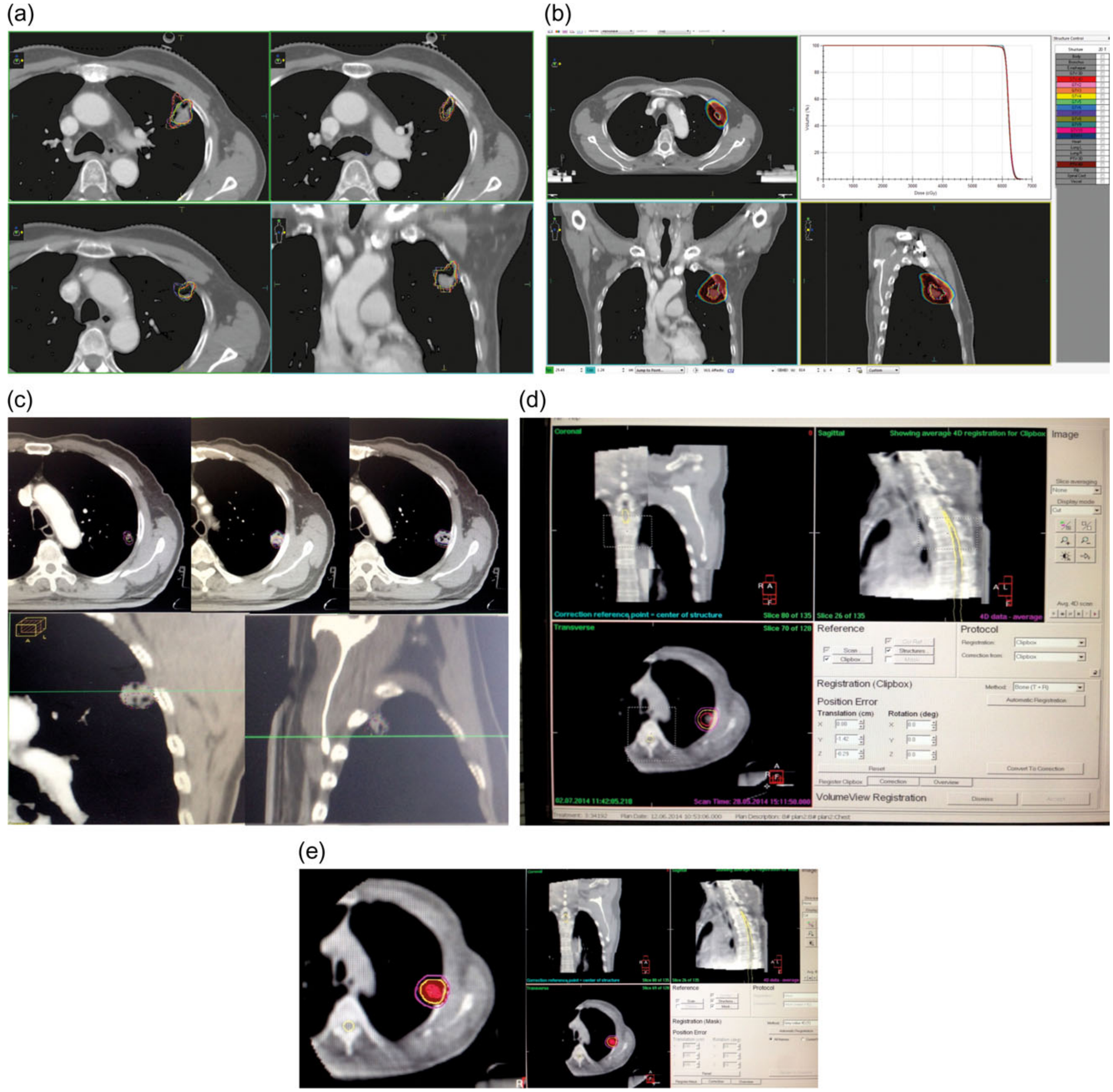

Fig. 2. (a) Case 1: The gross tumor volume (GTV) was outlined in each of 10 sequence images acquired by 4D-CT, as indicated by the different colored lines, and was projected onto the end-expiratory phase sequence. The internal motion of the tumor could be observed. (b) Case 1: Monte Carlo dose calculation was performed on the end-expiratory phase sequence to obtain the required dose. (c) Case 2: The GTV was outlined in 10 sequence images as indicated by the different colored lines. (d) Case 2: A clip box (white dashed box seen in sagittal plane, frontal plane and transverse section) was used to select the vertebral body on the layer corresponding to the tumor (seen in transverse section) as the region of interest (ROI). Next, automatic bone registration was performed for the 4D-CBCT end-expiratory phase sequences or 3D-CBCT and 4D-CT end-expiratory phase sequences. (e) Case 2: the mask function (the red region almost overlaps with the ITV region) was used to select images within the ITV region (contoured by yellow line around the tumor; the purple line indicates the PTV) as the ROI, and automatic soft-tissue registration was performed.

In this study, 4D-CBCT showed superior image guidance, and the possible reasons for this finding are as follows. First, the composite image sequences of 4D-CBCT and ITV were used for registration, and both can accurately show the internal motion of the tumors. In contrast, although 3D-CBCT can approximate the trajectory of the tumor during respiratory movements, it is akin to

Table 2. Range of internal motion of tumors in three dimensions

	Average (mm)	Standard deviation (mm)	Minimum (mm)	Maximum (mm)
LR	3.50	±0.54	2.3	4.5
SI	10.67	±2.61	6.8	14.5
AP	5.25	±1.75	2.8	7.7
3D vector	12.52	±2.65	7.7	16.6

LR = left-right direction, SI = superior–inferior direction, AP = anterior–posterior direction.

Table 3. Errors of image-guided registration based on 4D-CBCT and 3D-CBCT

	LR	SI	AP	3D vector
4D-CBCT (mm)	0.80 ± 0.21	2.02 ± 0.46	0.52 ± 0.16	2.25 ± 0.44
3D-CBCT (mm)	1.08 ± 0.25	3.30 ± 0.53	0.85 ± 0.24	3.59 ± 0.48
P-value	<0.001	<0.001	<0.001	<0.001

'capturing a fast-moving object with a slow shutter'. Though the image quality of both 4D-CBCT and 3D-CBCT in this study enabled us to complete the process of registration without difficulties, as is indicated, significantly worse image quality was observed in 3D-CBCT compared with 4D-CBCT, and the poor imaging quality had a significant impact on the accuracy of image guidance [7]. Second, the tumors in this group of patients showed a broad range of internal motion; hence, large discrepancies were noted in the data collected between using 4D-CBCT and 3D-CBCT, which demonstrates the advantage of 4D-CBCT in image guidance. Third, automatic registration was used in this study to reduce the interference of human factors. It is noteworthy that when calculating the error in 3D-CBCT image guidance, the displaced 4D-CBCT end-expiratory phase was used as a reference. The underlying assumption was that 3D-CBCT and 4D-CBCT acquisition were performed at an identical spatiotemporal location; however, in reality, the patient might have moved slightly between the two acquisition processes, which could influence the judgement of error in 3D-CBCT image guidance to a certain extent.

This study has some limitations. First, the accuracy of the radiotherapy is ultimately reflected in the implementation of the dose calculation results during the actual radiotherapy on the tumor and surrounding normal tissue; however, the XVI software system is still unable to implement image guidance based on dosimetry. Second, the slice thickness of CT and CBCT are important factors influencing the accuracy of image fusion. It was indicated that smaller slice thickness and larger lesions produced more accurate volume assessment than larger slice thickness and smaller lesions [39]. Due to the limitations of the facilities, a slice thickness of 3 mm is the thinnest one that can currently be achieved. It can be predicted that a more desirable result could be obtained if thinner slice thickness were available. Third, since this study mainly focused on whether 4D-CBCT enhances the accuracy of registration for small lesions in lungs (from the perspective of clinical practice), the physics of the technique (including phantom study and image quality) requires further investigation. In addition, the images acquired by 4D-CBCT and 3D-CBCT represent the movements of the tumor and surrounding normal tissue before the actual irradiation process; however, tumor motion during radiotherapy might be different from that during image guidance performed before radiotherapy. Furthermore, the small sample size of this study might have introduced bias.

CONCLUSION

In summary, 4D-CBCT might be better than 3D-CBCT for image guidance in small pulmonary tumor irradiation. This is because 4D-CBCT can reduce the unreliability of radiation delivery resulting from the internal motion caused by respiratory movements during image guidance, thereby increasing the accuracy of image guidance. However, this requires further investigation in a study with a larger patient population.

ACKNOWLEDGEMENTS

We thank Yangkun Luo for valuable discussion on the design of the protocol, Chuandong Cheng for assistance with registration, and Lintao Li for assistance with image acquisition.

CONFLICT OF INTEREST

We declare that we have no financial or personal relationships with other people or organizations that might inappropriately influence our work, and there is no professional or other personal interest of any nature or kind in any product, service and/or company that could be construed as influencing the position presented in, or the review of, this manuscript.

FUNDING

None.

REFERENCES

1. Henschke CI, McCauley DI, Yankelevitz DF et al. Early Lung Cancer Action Project: overall design and findings from baseline screening. *Lancet* 1999;354:99–105.
2. Henschke CI, Naidich DP, Yankelevitz DF et al. Early lung cancer action project: initial findings on repeat screenings. *Cancer* 2001;92:153–9.
3. Kaneko M, Kusumoto M, Kobayashi T et al. Computed tomography screening for lung carcinoma in Japan. *Cancer* 2000;89: 2485–8.
4. Timmerman R, Paulus R, Galvin J et al. Stereotactic body radiation therapy for inoperable early stage lung cancer. *JAMA* 2010;303:1070–6.
5. Guckenberger M, Krieger T, Richter A et al. Potential of image-guidance, gating and real-time tracking to improve accuracy in

pulmonary stereotactic body radiotherapy. *Radiother Oncol* 2009;91:288–95.
6. Seppenwoolde Y, Shirato H, Kitamura K et al. Precise and real-time measurement of 3D tumor motion in lung due to breathing and heartbeat, measured during radiotherapy. *Int J Radiat Oncol Biol Phys* 2002;53:822–34.
7. Sweeney RA, Seubert B, Stark S et al. Accuracy and inter-observer variability of 3D versus 4D cone-beam CT based image-guidance in SBRT for lung tumors. *Radiat Oncol* 2012;7:81.
8. Sonke JJ, Zijp L, Remeijer P et al. Respiratory correlated cone beam CT. *Med Phys* 2005;32:1176–86.
9. Hugo GD, Liang J, Campbell J et al. On-line target position localization in the presence of respiration: a comparison of two methods. *Int J Radiat Oncol Biol Phys* 2007;69:1634–41.
10. Nakagawa K, Haga A, Kida S et al. 4D registration and 4D verification of lung tumor position for stereotactic volumetric modulated arc therapy using respiratory-correlated cone-beam CT. *J Radiat Res* 2013;54:152–6.
11. Nakagawa K, Kida S, Haga A et al. 4D digitally reconstructed radiography for verifying a lung tumor position during volumetric modulated arc therapy. *J Radiat Res* 2012;53:628–32.
12. Bissonnette JP, Franks KN, Purdie TG et al. Quantifying interfraction and intrafraction tumor motion in lung stereotactic body radiotherapy using respiration-correlated cone beam computed tomography. *Int J Radiat Oncol Biol Phys* 2009;75:688–95.
13. Sonke JJ, Rossi M, Wolthaus J et al. Frameless stereotactic body radiotherapy for lung cancer using four-dimensional cone beam CT guidance. *Int J Radiat Oncol Biol Phys* 2009;74:567–74.
14. Gao H, Li R, Lin Y et al. 4D cone beam CT via spatiotemporal tensor framelet. *Med Phys* 2012;39:6943–6.
15. Wong JW, Sharpe MB, Jaffray DA et al. The use of active breathing control (ABC) to reduce margin for breathing motion. *Int J Radiat Oncol Biol Phys* 1999;44:911–19.
16. Ohara K, Okumura T, Akisada M et al. Irradiation synchronized with respiration gate. *Int J Radiat Oncol Biol Phys* 1989;17:853–7.
17. Hurkmans CW, van Lieshout M, Schuring D et al. Quality assurance of 4D-CT scan techniques in multicenter phase III trial of surgery versus stereotactic radiotherapy (radiosurgery or surgery for operable early stage (stage 1A) non-small-cell lung cancer [ROSEL] study). *Int J Radiat Oncol Biol Phys* 2011;80:918–27.
18. Richter A, Wilbert J, Baier K et al. Feasibility study for markerless tracking of lung tumors in stereotactic body radiotherapy. *Int J Radiat Oncol Biol Phys* 2010;78:618–27.
19. Korreman S, Persson G, Nygaard D et al. Respiration-correlated image guidance is the most important radiotherapy motion management strategy for most lung cancer patients. *Int J Radiat Oncol Biol Phys* 2012;83:1338–43.
20. Howington JA, Blum MG, Chang AC et al. Treatment of stage I and II non-small cell lung cancer: diagnosis and management of lung cancer, 3rd ed: American College of Chest Physicians evidence-based clinical practice guidelines. *Chest* 2013;143:e278S–313S.
21. Bilal H, Mahmood S, Rajashanker B et al. Is radiofrequency ablation more effective than stereotactic ablative radiotherapy in patients with early stage medically inoperable non-small cell lung cancer? *Interact Cardiovasc Thorac Surg* 2012;15:258–65.
22. Shirvani SM, Jiang J, Chang JY et al. Comparative effectiveness of 5 treatment strategies for early-stage non-small cell lung cancer in the elderly. *Int J Radiat Oncol Biol Phys* 2012;84:1060–70.
23. Grutters JP, Kessels AG, Pijls-Johannesma M et al. Comparison of the effectiveness of radiotherapy with photons, protons and carbon-ions for non-small cell lung cancer: a meta-analysis. *Radiother Oncol* 2010;95:32–40.
24. Baumann P, Nyman J, Hoyer M et al. Outcome in a prospective phase II trial of medically inoperable stage I non-small-cell lung cancer patients treated with stereotactic body radiotherapy. *J Clin Oncol* 2009;27:3290–6.
25. Palma D, Visser O, Lagerwaard FJ et al. Impact of introducing stereotactic lung radiotherapy for elderly patients with stage I non-small-cell lung cancer: a population-based time-trend analysis. *J Clin Oncol* 2010;28:5153–9.
26. Widder J, Postmus D, Ubbels JF et al. Survival and quality of life after stereotactic or 3D-conformal radiotherapy for inoperable early-stage lung cancer. *Int J Radiat Oncol Biol Phys* 2011;81:e291–7.
27. Bradley JD, El Naqa I, Drzymala RE et al. Stereotactic body radiation therapy for early-stage non-small-cell lung cancer: the pattern of failure is distant. *Int J Radiat Oncol Biol Phys* 2010;77:1146–50.
28. Senthi S, Lagerwaard FJ, Haasbeek CJ et al. Patterns of disease recurrence after stereotactic ablative radiotherapy for early stage non-small-cell lung cancer: a retrospective analysis. *Lancet Oncol* 2012;13:802–9.
29. Fakiris AJ, McGarry RC, Yiannoutsos CT et al. Stereotactic body radiation therapy for early-stage non-small-cell lung carcinoma: four-year results of a prospective phase II study. *Int J Radiat Oncol Biol Phys* 2009;75:677–82.
30. Donington J, Ferguson M, Mazzone P et al. American College of Chest Physicians and Society of Thoracic Surgeons consensus statement for evaluation and management for high-risk patients with stage I non-small cell lung cancer. *Chest* 2012;142:1620–35.
31. Guckenberger M, Andratschke N, Alheit H et al. Definition of stereotactic body radiotherapy: principles and practice for the treatment of stage I non-small cell lung cancer. *Strahlenther Onkol* 2014;190:26–33.
32. Onishi H, Shirato H, Nagata Y et al. Stereotactic body radiotherapy (SBRT) for operable stage I non-small-cell lung cancer: can SBRT be comparable to surgery? *Int J Radiat Oncol Biol Phys* 2011;81:1352–8.
33. Iyengar P, Westover K, Timmerman RD. Stereotactic ablative radiotherapy (SABR) for non-small cell lung cancer. *Semin Respir Crit Care Med* 2013;34:845–54.
34. Rosenzweig KE, Chang JY, Chetty IJ et al. ACR appropriateness criteria nonsurgical treatment for non-small-cell lung cancer: poor performance status or palliative intent. *J Am Coll Radiol* 2013;10:654–64.
35. Taremi M, Hope A, Dahele M et al. Stereotactic body radiotherapy for medically inoperable lung cancer: prospective,

single-center study of 108 consecutive patients. *Int J Radiat Oncol Biol Phys* 2012;82:967–73.

36. Dahele M, Senan S. The role of stereotactic ablative radiotherapy for early-stage and oligometastatic non-small cell lung cancer: evidence for changing paradigms. *Cancer Res Treat* 2011; 43:75–82.
37. Heinzerling JH, Kavanagh B, Timmerman RD. Stereotactic ablative radiation therapy for primary lung tumors. *Cancer J* 2011;17:28–32.
38. Potters L, Kavanagh B, Galvin JM et al. American Society for Therapeutic Radiology and Oncology (ASTRO) and American College of Radiology (ACR) practice guideline for the performance of stereotactic body radiation therapy. *Int J Radiat Oncol Biol Phys* 2010;76:326–32.
39. Prionas ND, Ray S, Boone JM. Volume assessment accuracy in computed tomography: a phantom study. *J Appl Clin Med Phys* 2010;11:3037.